Available online at www.sciencedirect.com
SCIENCE DIRECT®
International Journal of Solids and Structures 43 (2006) 5055–5065
INTERNATIONAL JOURNAL OF SOLIDS and STRUCTURES
www.elsevier.com/locate/ijsolstr

Size dependent, non-uniform elastic field inside a nano-scale spherical inclusion due to interface stress

C.W. Lim [a,*], Z.R. Li [a], L.H. He [b]

[a] Department of Building and Construction, City University of Hong Kong, Tat Chee Avenue, Kowloon, Hong Kong
[b] Key Laboratory of Mechanical Behavior and Design of Materials, CAS, University of Science and Technology of China, Hefei, Anhui, PR China

Received 14 April 2005
Available online 28 September 2005

Abstract

The primary objective of the present paper is to analyze the influence of interface stress on the elastic field within a nano-scale inclusion. Special attention is focused on the case of non-hydrostatic eigenstrain. From the viewpoint of practicality, it is assumed that the inclusion is spherically shaped and embedded into an infinite solid, within which an axisymmetric eigenstrain is prescribed. Following Goodier's work, the elastic fields inside and outside the inclusion are obtained analytically. It is found that the presence of interface stress leads to conclusion that the elastic field in the inclusion is not only dependent on inclusion size but also on non-uniformity. The result is in strong contrast to Eshelby's solution based on classical elasticity, and it is helpful in the understanding of relevant physical phenomena in nano-structured solids.

Keywords: Interface stress; Spherical inclusion; Size effect

1. Introduction

Analysis of elastic stress in an inclusion or an inhomogeneity is a classical problem in solid mechanics and physics (Mura, 1987). The famous work by Eshelby (1957) indicates that the resulting elastic field inside an ellipsoid inclusion with a uniform eigenstrain embedded into an infinite solid is still uniform. Such an elegant result provides a sound basis to micromechanics of materials. Recently, the problem of elastic inclusions has drawn renewed interest due to the rapid development of nanotechnology. An important example is the estimation of stresses due to lattice mismatch in buried quantum dots which can be used to tailor band-gap structures of the dots so as to improve the performance of the relevant photoelectronic devices (Bimberg et al., 1999). Typically, the size of a quantum dot is well below 100 nm. An unusual feature in this case is that the elastic field in the small inclusion is significantly influenced by the interface stress. Indeed, interface is effectively an idealization of the special region with small thickness between two phases in an inhomogeneous solid. For inclusions

* Corresponding author. Tel.: +852 2788 7285; fax: +852 2788 7612.
E-mail address: bccwlim@cityu.edu.hk (C.W. Lim).

0020-7683/$ - see front matter © 2005 Elsevier Ltd. All rights reserved.
doi:10.1016/j.ijsolstr.2005.08.007

of large size, the effect of interface stress can be ignored, as in the case studied by Eshelby (1957); for inclusions of small size, such as quantum dots, the effect of interface stress may be quite remarkable because of the increased contribution to the total energy from the interface. The same conclusion applies equally for the effect of surface stress in nano-scale solids as well. Evidence in both experiments (Wong et al., 1997; Rose et al., 2000) and theory (Sun and Zhang, 2003; Zhou and Huang, 2004) exist which reveal that the deformation behavior of elastic elements with nano-scale characteristic dimension is essentially size dependent.

A generic and mathematical exposition on surface/interface elasticity has been presented by Gurtin and his co-workers (Gurtin and Murdoch, 1975; Gurtin et al., 1998). In their work, a surface/interface is regarded as a negligibly thin object adhering to the bulk without slipping. The material constants of the surface/interface are different from the bulk materials. The equilibrium and constitutive equations of the bulk solid are the same as those in the classical elasticity, but the presence of surface/interface stress gives rise to a non-classical boundary condition. Utilizing this model, Miller and Shenoy (2000) examined unidirectional tension and pure bending of nano-scale bars and plates. The results are in excellent agreement with their atomistic simulation by embedded atom method for face-centered cubic aluminum and the Stillinger–Weber model for silicon. They thus concluded that the size-dependent deformation of elastic elements with nano-scale dimensions can be referred to the effect of surface/interface stresses. Recently, a general model for ultrathin elastic films with nano-scale thickness was developed by He et al. (2004) rigorously from three-dimensional elasticity coupled with the surface model proposed by Gurtin and Murdoch (1975). As to nano-scale inclusions, Sharma and his co-workers (Sharma and Ganti, 2002; Sharma et al., 2003) provided analytical expressions for the size-dependent strain states caused by nano-inhomogeneities (including spherical quantum dots and pores), showing that surface/interface stress can significantly alter the fundamental nature of stress state at nanometer length scales. Moreover, Sharma and Ganti (2004) presented a general formulation for size-dependent Eshelby's tensor for embedded nano-inclusions by taking account of surface/interface energies, and found that only inclusions that are of a constant curvature admit a uniform elastic state. In their papers, however, explicit results are presented only for equiaxial stress case. Yang (2004) attempted to examine the effect of the surface energy (independent of deformation) on the effective modulus of an elastic composite material containing spherical nano-cavities and found the effective shear modulus and bulk modulus are not only size dependent but also strain dependent. As pointed out by Sun et al. (2004), a constant surface stress independent of the elastic strain should have no influence on the effective shear modulus. The main result in Yang (2004) should be reexamined.

The purpose of this paper is to examine the effect of interface effect on the elastic state of spherical inclusion with uniform, non-hydrostatic axisymmetric eigenstrains. Following the work of Goodier (1933), an analytical solution is obtained for the elastic state of spherical inclusion coupled with interface effect. The result indicates that the presence of interface stress leads to size dependence of the elastic field, and in addition, to non-uniformity of the stress and strain inside the inclusion even though the inclusion is of a constant curvature. This conclusion is in strong contrast with that predicted by the classical elasticity theory, and it can be regarded as complementary to the analysis of Sharma and Ganti's work (2004).

2. Formulation of the problem

In the framework of continuum model, the interface region of a body can be modeled as a material surface adhering to the body without slipping. The infinitesimal deformation in the interior of an elastically isotropic body is described by the common equations (Mura, 1987) as

$$\begin{aligned} &\nabla \cdot \boldsymbol{\sigma} = \mathbf{0}, \\ &\boldsymbol{\sigma} = 2\mu(\boldsymbol{\varepsilon} - \boldsymbol{\varepsilon}^*) + \lambda[\mathrm{tr}(\boldsymbol{\varepsilon} - \boldsymbol{\varepsilon}^*)]\mathbf{I}, \\ &\boldsymbol{\varepsilon} = \frac{1}{2}\left[\nabla \mathbf{u} + (\nabla \mathbf{u})^{\mathrm{T}}\right], \end{aligned} \tag{1}$$

where ∇ is the gradient operator, $\boldsymbol{\sigma}$, $\boldsymbol{\varepsilon}$ and $\mathbf{u}$ denote, respectively, stress, strain and displacement, $\boldsymbol{\varepsilon}^*$ is eigenstrain, λ and μ are Lamé constants, and $\mathbf{I}$ the unity tensor. The interface has its own elastic properties and is characterized by (Gurtin and Murdoch, 1975):

$$\begin{aligned}
&\nabla_\Sigma \cdot \mathbf{\Sigma} = \boldsymbol{\sigma} \cdot \mathbf{n},\\
&\mathbf{\Sigma} = \tau_0 \mathbf{I}_\Sigma + 2(\mu_0 - \tau_0)\mathbf{I}_\Sigma \mathbf{E} + (\lambda_0 + \tau_0)(\mathrm{tr}\mathbf{E})\mathbf{I}_\Sigma + \tau_0 \nabla_\Sigma \mathbf{u},\\
&\mathbf{E} = \frac{1}{2}\left[D\mathbf{u} + (D\mathbf{u})^{\mathrm{T}}\right],
\end{aligned} \tag{2}$$

in which $\mathbf{\Sigma}$ and $\mathbf{E}$ are interface stress and interface strain, τ_0 is interfacial tension, $\mathbf{n}$ is the outward unit vector normal to the interface, λ_0 and μ_0 are interfacial Lamé constants, $\mathbf{I}_\Sigma$ and ∇_Σ are unity tensor and gradient operator, respectively, defined on the interface, and $D\mathbf{u} = (\mathbf{I} - \mathbf{n} \otimes \mathbf{n}) \cdot \nabla_\Sigma \mathbf{u}$ where $\otimes$ denotes tensor product. Note that the last term in the second equation in Eq. (2), $\tau_0 \nabla_\Sigma \mathbf{u}$, is often omitted in some published studies (Sharma and Ganti, 2002; Sharma et al., 2003).

The problem considered in this paper is a spherical inclusion of radius R embedded in an infinite elastic body, as shown in Fig. 1. An axisymmetric eigenstrain $\boldsymbol{\varepsilon}^* = \varepsilon^*_{11}\mathbf{e}_1 \otimes \mathbf{e}_1 + \varepsilon^*_{11}\mathbf{e}_2 \otimes \mathbf{e}_2 + \varepsilon^*_{33}\mathbf{e}_3 \otimes \mathbf{e}_3$ is given in the inclusion, where $\mathbf{e}_1$, $\mathbf{e}_2$ and $\mathbf{e}_3$ are, respectively, the base vectors along the x_1, x_2 and x_3 directions. It is convenient to carry out the analysis in spherical coordinates (r–θ–φ) with the origin at the center of the inclusion. For simplicity, both the matrix and inclusion are assumed elastically isotropic with the same elastic modulus. Since the deformation is axisymmetric about the x_3-axis, the displacements will be confined to meridian planes, having a component u_r along the radius r, and a component u_θ in the direction of increasing θ. Within and outside the sphere, the displacement, $\mathbf{u} = u_r\mathbf{e}_r + u_\theta\mathbf{e}_\theta$, satisfies the following Navier's equation (with no body forces):

$$(1 + \Lambda)\nabla(\nabla \cdot \mathbf{u}) + \nabla^2 \mathbf{u} = \mathbf{0}, \tag{3}$$

with $\Lambda = \lambda/\mu$ and $\nabla = \mathbf{e}_r(\partial/\partial r) + \mathbf{e}_\theta(\partial/r\partial\theta)$, where $\mathbf{e}_r$, $\mathbf{e}_\varphi$ and $\mathbf{e}_\theta$ are base vectors along the respect coordinates. The general formulas for the non-zero strains are

$$\boldsymbol{\varepsilon} = \frac{\partial u_r}{\partial r}\mathbf{e}_r \otimes \mathbf{e}_r + \left(\frac{1}{r}\frac{\partial u_r}{\partial \theta} + \frac{\partial u_\theta}{\partial r} - \frac{u_\theta}{r}\right)\mathbf{e}_r \otimes \mathbf{e}_\theta + \left(\frac{1}{r}\frac{\partial u_\theta}{\partial \theta} + \frac{u_r}{r}\right)\mathbf{e}_\theta \otimes \mathbf{e}_\theta + \frac{1}{r}(u_r + u_\theta \cot\theta)\mathbf{e}_\varphi \otimes \mathbf{e}_\varphi. \tag{4}$$

According to Hooke's law, the corresponding non-zero stress is

$$\begin{aligned}
\boldsymbol{\sigma} = {} & \mu\left(\Lambda\nabla \cdot \mathbf{u} + 2\frac{\partial u_r}{\partial r}\right)\mathbf{e}_r \otimes \mathbf{e}_r + \mu\left(\frac{1}{r}\frac{\partial u_r}{\partial \theta} + \frac{\partial u_\theta}{\partial r} - \frac{u_\theta}{r}\right)\mathbf{e}_r \otimes \mathbf{e}_\theta\\
& + \mu\left[\Lambda\nabla \cdot \mathbf{u} + \frac{2}{r}(u_r + u_\theta \cot\theta)\right]\mathbf{e}_\varphi \otimes \mathbf{e}_\varphi + \mu\left[\Lambda\nabla \cdot \mathbf{u} + \frac{2}{r}\left(\frac{\partial u_\theta}{\partial \theta} + u_r\right)\right]\mathbf{e}_\theta \otimes \mathbf{e}_\theta.
\end{aligned} \tag{5}$$

This stress field must fulfills

$$\begin{aligned}
[\![\sigma_{rr}]\!]\mathbf{e}_r \otimes \mathbf{e}_r + [\![\sigma_{r\theta}]\!]\mathbf{e}_r \otimes \mathbf{e}_\theta = {} & -\frac{1}{R}\left[\frac{\partial \mathbf{\Sigma}_{r\theta}}{\partial \theta} - \left(\mathbf{\Sigma}_{\varphi\varphi} + \mathbf{\Sigma}_{\theta\theta}\right) + \Sigma_{r\theta}\cot\theta\right]\mathbf{e}_r \otimes \mathbf{e}_r\\
& - \frac{1}{R}\left[\frac{\partial \Sigma_{\theta\theta}}{\partial \theta} + \Sigma_{r\theta} - \left(\Sigma_{\varphi\varphi} - \Sigma_{\theta\theta}\right)\cot\theta\right]\mathbf{e}_r \otimes \mathbf{e}_\theta
\end{aligned} \tag{6}$$

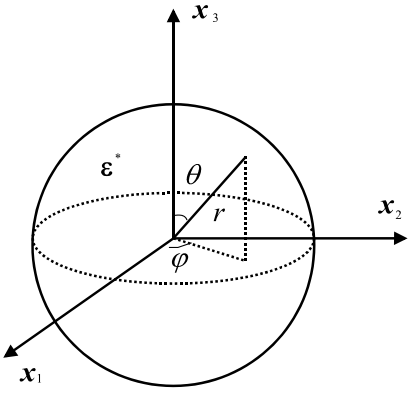

Fig. 1. Spherical inclusion with uniform axisymmetric eigenstrain embedded in an infinite matrix.

at $r = R$, where $[\![\sigma_{ij}]\!] = \sigma_{ij}(R^+) - \sigma_{ij}(R^-)$ denotes the jump of the stress at the interface. Here the interface stress tensor is written as

$$\boldsymbol{\Sigma} = \tau_0\left(\frac{1}{R}\frac{\partial u_r}{\partial\theta} - \frac{u_\theta}{R}\right)\mathbf{e}_r \otimes \mathbf{e}_\theta + \left\{\tau_0 + [2(\lambda_0+\mu_0)+\tau_0]\frac{u_r}{R} + (\lambda_0+\tau_0)\frac{u_\theta}{R}\cot\theta + (\lambda_0+2\mu_0)\frac{1}{R}\frac{\partial u_\theta}{\partial\theta}\right\}\mathbf{e}_\theta \otimes \mathbf{e}_\theta + \left\{\tau_0 + [2(\lambda_0+\mu_0)+\tau_0]\frac{u_r}{R} + (\lambda_0+2\mu_0)\frac{u_\theta}{R}\cot\theta + (\lambda_0+\tau_0)\frac{1}{R}\frac{\partial u_\theta}{\partial\theta}\right\}\mathbf{e}_\varphi \otimes \mathbf{e}_\varphi. \tag{7}$$

3. Solution of the problem

The solution to Eq. (3) can be expressed in terms of two types of spherical solid harmonical functions (Goodier, 1933; Love, 1944), ϕ, ω_n, as

$$\mathbf{u} = \left[\frac{\partial\phi}{\partial r} + \left(r^2\frac{\partial\omega_n}{\partial r} + \alpha_n r\omega_n\right)\right]\mathbf{e}_r + \left(\frac{1}{r}\frac{\partial\phi}{\partial\theta} + r\frac{\partial\omega_n}{\partial\theta}\right)\mathbf{e}_\theta, \tag{8}$$

with

$$\nabla^2\phi = 0, \quad \nabla^2\omega_n = 0, \tag{9}$$

where the value of α_n is given by

$$\alpha_n = -2\frac{3n+1+n\Lambda}{n+5+(n+3)\Lambda}. \tag{10}$$

The general axisymmetric solution of Eq. (9) is of the form

$$\Sigma_{n=0}^{\infty}\left(b_n r^n + \frac{c_n}{r^{n+1}}\right)P_n(\cos\theta), \tag{11}$$

where $P_n(\cos\theta)$ is the Legendre polynomial, with $P_0(x) = 1$, $P_1(x) = x$ and $P_2(x) = (3x^2-1)/2$, etc. For the region outside the inclusion, ϕ and ω_n can take the following special forms

$$\phi = \frac{c_0}{r} + \frac{c_2}{r^3}P_2(\cos\theta), \quad \omega_{-3} = \frac{c_2'}{r^3}P_2(\cos\theta) \tag{12}$$

and within the inclusion, ϕ and ω_n are of the form

$$\phi = b_2 r^2 P_2(\cos\theta), \quad \omega_2 = b_2' r^2 P_2(\cos\theta), \quad \omega_0 = b_0 \tag{13}$$

in which b_0, b_2, b_2', c_0, c_2 and c_2' are constants to be determined.

The continuity condition for displacements together with the equilibrium condition (6) at $r = R$ yield six independent equations which demand

$$\begin{aligned} &\frac{c_0}{R^3} = \xi_0\varepsilon^* + \chi_0\frac{\tau_0}{\mu R}, \quad \frac{c_2}{R^5} = \xi_1\varepsilon^*, \quad \frac{c_2'}{R^3} = \xi_2\varepsilon^*, \\ &b_0 = \eta_0\varepsilon^* + \chi_1\frac{\tau_0}{\mu R}, \quad b_2 = \eta_1\varepsilon^*, \quad b_2'R^2 = \eta_2\varepsilon^*, \end{aligned} \tag{14}$$

where ξ_0, ξ_1, ξ_2, η_0, η_1, η_2, χ_0 and χ_1 are dimensionless constants depending not only on the bulk and interface material properties of the elastic body but also on the radius of inclusion. The explicit expressions of these constants are given in Appendix. Therefore, invoking the results in Eqs. (12)–(14), the displacement field of the infinite elastic matrix is obtained as

$$\begin{aligned} u_r = &-\frac{\chi_0\tau_0}{\mu}\left(\frac{R}{r}\right)^2 - r\left\{\left(\varepsilon_{33}^* + 2\varepsilon_{11}^*\right)\xi_0\left(\frac{R}{r}\right)^3 + \left(\varepsilon_{33}^* - \varepsilon_{11}^*\right)\left[\frac{3}{4}\xi_1\left(\frac{R}{r}\right)^5 - \frac{5+3\Lambda}{4}\xi_2\left(\frac{R}{r}\right)^3\right]\right\} \\ &- r\left(\varepsilon_{33}^* - \varepsilon_{11}^*\right)\left[\frac{9}{4}\xi_1\left(\frac{R}{r}\right)^5 - \frac{3(5+3\Lambda)}{4}\xi_2\left(\frac{R}{r}\right)^3\right]\cos 2\theta, \\ u_\theta = &-r\left(\varepsilon_{33}^* - \varepsilon_{11}^*\right)\left[\frac{3}{2}\xi_1\left(\frac{R}{r}\right)^5 + \frac{3}{2}\xi_2\left(\frac{R}{r}\right)^3\right]\sin 2\theta \end{aligned} \tag{15}$$

and the relevant strain and stress fields read

$$\begin{aligned}
\varepsilon_{rr} &= \frac{2\chi_0\tau_0}{\mu R}\left(\frac{R}{r}\right)^3 + \left\{2\left(\varepsilon_{33}^* + 2\varepsilon_{11}^*\right)\xi_0\left(\frac{R}{r}\right)^3 + \left(\varepsilon_{33}^* - \varepsilon_{11}^*\right)\left[3\xi_1\left(\frac{R}{r}\right)^5 - \frac{5+3\Lambda}{2}\xi_2\left(\frac{R}{r}\right)^3\right]\right\} \\
&\quad + \left(\varepsilon_{33}^* - \varepsilon_{11}^*\right)\left[9\xi_1\left(\frac{R}{r}\right)^5 - \frac{3(5+3\Lambda)}{2}\xi_2\left(\frac{R}{r}\right)^3\right]\cos 2\theta, \\
\varepsilon_{\theta\theta} &= -\frac{\chi_0\tau_0}{\mu R}\left(\frac{R}{r}\right)^3 - \left\{\left(\varepsilon_{33}^* + 2\varepsilon_{11}^*\right)\xi_0\left(\frac{R}{r}\right)^3 + \left(\varepsilon_{33}^* - \varepsilon_{11}^*\right)\left[\frac{3}{4}\xi_1\left(\frac{R}{r}\right)^5 - \frac{5+3\Lambda}{4}\xi_2\left(\frac{R}{r}\right)^3\right]\right\} \\
&\quad - \left(\varepsilon_{33}^* - \varepsilon_{11}^*\right)\left[\frac{21}{4}\xi_1\left(\frac{R}{r}\right)^5 - \frac{3+9\Lambda}{4}\xi_2\left(\frac{R}{r}\right)^3\right], \\
\varepsilon_{\varphi\varphi} &= -\frac{\chi_0\tau_0}{\mu R}\left(\frac{R}{r}\right)^3 - \left\{\left(\varepsilon_{33}^* + 2\varepsilon_{11}^*\right)\xi_0\left(\frac{R}{r}\right)^3 + \left(\varepsilon_{33}^* - \varepsilon_{11}^*\right)\left[\frac{9}{4}\xi_1\left(\frac{R}{r}\right)^5 + \frac{1-3\Lambda}{4}\xi_2\left(\frac{R}{r}\right)^3\right]\right\} \\
&\quad - \left(\varepsilon_{33}^* - \varepsilon_{11}^*\right)\left[\frac{15}{4}\xi_1\left(\frac{R}{r}\right)^5 - \frac{9(1+\Lambda)}{4}\xi_2\left(\frac{R}{r}\right)^3\right], \\
\varepsilon_{r\theta} &= \left(\varepsilon_{33}^* - \varepsilon_{11}^*\right)\left[12\xi_1\left(\frac{R}{r}\right)^5 - \frac{3(2+3\Lambda)}{2}\xi_2\left(\frac{R}{r}\right)^3\right]
\end{aligned} \tag{16}$$

and

$$\begin{aligned}
\sigma_{rr} &= \frac{4\chi_0\tau_0}{R}\left(\frac{R}{r}\right)^3 + \mu\left\{4\left(\varepsilon_{33}^* + 2\varepsilon_{11}^*\right)\xi_0\left(\frac{R}{r}\right)^3 + \left(\varepsilon_{33}^* - \varepsilon_{11}^*\right)\left[6\xi_1\left(\frac{R}{r}\right)^5 - \frac{10+9\Lambda}{2}\xi_2\left(\frac{R}{r}\right)^3\right]\right\} \\
&\quad + \mu\left(\varepsilon_{33}^* - \varepsilon_{11}^*\right)\left[18\xi_1\left(\frac{R}{r}\right)^5 - \frac{3(10+9\Lambda)}{2}\xi_2\left(\frac{R}{r}\right)^3\right]\cos 2\theta, \\
\sigma_{\theta\theta} &= -\frac{2\chi_0\tau_0}{R}\left(\frac{R}{r}\right)^3 - \mu\left\{2\left(\varepsilon_{33}^* + 2\varepsilon_{11}^*\right)\xi_0\left(\frac{R}{r}\right)^3 + \left(\varepsilon_{33}^* - \varepsilon_{11}^*\right)\left[\frac{3}{2}\xi_1\left(\frac{R}{r}\right)^5 - \frac{5}{2}\xi_2\left(\frac{R}{r}\right)^3\right]\right\} \\
&\quad - \mu\left(\varepsilon_{33}^* - \varepsilon_{11}^*\right)\left[\frac{21}{2}\xi_1\left(\frac{R}{r}\right)^5 - \frac{3}{2}\xi_2\left(\frac{R}{r}\right)^3\right]\cos 2\theta, \\
\sigma_{\varphi\varphi} &= -\frac{2\chi_0\tau_0}{R}\left(\frac{R}{r}\right)^3 - \mu\left\{2\left(\varepsilon_{33}^* + 2\varepsilon_{11}^*\right)\xi_0\left(\frac{R}{r}\right)^3 + \left(\varepsilon_{33}^* - \varepsilon_{11}^*\right)\left[\frac{9}{2}\xi_1\left(\frac{R}{r}\right)^5 + \frac{1}{2}\xi_2\left(\frac{R}{r}\right)^3\right]\right\} \\
&\quad - \mu\left(\varepsilon_{33}^* - \varepsilon_{11}^*\right)\left[\frac{15}{2}\xi_1\left(\frac{R}{r}\right)^5 - \frac{9}{2}\xi_2\left(\frac{R}{r}\right)^3\right]\cos 2\theta, \\
\sigma_{r\theta} &= \mu\left(\varepsilon_{33}^* - \varepsilon_{11}^*\right)\left[12\xi_1\left(\frac{R}{r}\right)^5 - \frac{3(2+3\Lambda)}{2}\xi_2\left(\frac{R}{r}\right)^3\right]\sin 2\theta,
\end{aligned} \tag{17}$$

respectively.

Similarly, the displacement field in the inclusion is given as follows:

$$\begin{aligned}
u_r &= -\frac{2\chi_1\tau_0}{\mu(5+3\Lambda)}\frac{r}{R} + r\left\{-\frac{2\left(\varepsilon_{33}^* + 2\varepsilon_{11}^*\right)}{5+3\Lambda}\eta_0 + \left(\varepsilon_{33}^* - \varepsilon_{11}^*\right)\left[\frac{1}{2}\eta_1 + \frac{3\Lambda}{2(7+5\Lambda)}\eta_2\left(\frac{r}{R}\right)^2\right]\right\} \\
&\quad + r\left(\varepsilon_{33}^* - \varepsilon_{11}^*\right)\left[\frac{3}{2}\eta_1 + \frac{9\Lambda}{2(7+5\Lambda)}\eta_2\left(\frac{r}{R}\right)^2\right]\cos 2\theta, \\
u_\theta &= -r\left(\varepsilon_{33}^* - \varepsilon_{11}^*\right)\left[\frac{3}{2}\eta_1 + \frac{3}{2}\eta_2\left(\frac{r}{R}\right)^2\right]\sin 2\theta
\end{aligned} \tag{18}$$

and the strain and stress fields are

$$
\begin{aligned}
\varepsilon_{rr} &= -\frac{2}{5+3\Lambda}\frac{\chi_1\tau_0}{\mu R} - \left\{\frac{2\left(\varepsilon_{33}^{*}+2\varepsilon_{11}^{*}\right)}{5+3\Lambda}\eta_0 - \left(\varepsilon_{33}^{*}-\varepsilon_{11}^{*}\right)\left[\frac{\eta_1}{2}+\frac{9\Lambda\eta_2}{2(7+5\Lambda)}\left(\frac{r}{R}\right)^2\right]\right\} \\
&\quad + \left(\varepsilon_{33}^{*}-\varepsilon_{11}^{*}\right)\left[\frac{3}{2}\eta_1 - \frac{27\Lambda\eta_2}{2(7+5\Lambda)}\left(\frac{r}{R}\right)^2\right]\cos 2\theta, \\
\varepsilon_{\theta\theta} &= -\frac{2}{5+3\Lambda}\frac{\chi_1\tau_0}{\mu R} - \left\{\frac{2\left(\varepsilon_{33}^{*}+2\varepsilon_{11}^{*}\right)}{5+3\Lambda}\eta_0 - \left(\varepsilon_{33}^{*}-\varepsilon_{11}^{*}\right)\left[\frac{\eta_1}{2}+\frac{3\Lambda\eta_2}{2(7+5\Lambda)}\left(\frac{r}{R}\right)^2\right]\right\} \\
&\quad - \left(\varepsilon_{33}^{*}-\varepsilon_{11}^{*}\right)\left[\frac{3}{2}\eta_1 + \frac{7(2+\Lambda)\eta_2}{2(7+5\Lambda)}\left(\frac{r}{R}\right)^2\right]\cos 2\theta, \\
\varepsilon_{\varphi\varphi} &= -\frac{2}{5+3\Lambda}\frac{\chi_1\tau_0}{\mu R} - \left\{\frac{2\left(\varepsilon_{33}^{*}+2\varepsilon_{11}^{*}\right)}{5+3\Lambda}\eta_0 + \left(\varepsilon_{33}^{*}-\varepsilon_{11}^{*}\right)\left[\eta_1+\frac{3(7+4\Lambda)\eta_2}{2(7+5\Lambda)}\left(\frac{r}{R}\right)^2\right]\right\} \\
&\quad - \left(\varepsilon_{33}^{*}-\varepsilon_{11}^{*}\right)\frac{3(7+2\Lambda)\eta_2}{2(7+5\Lambda)}\left(\frac{r}{R}\right)^2\cos 2\theta, \\
\varepsilon_{r\theta} &= -\left(\varepsilon_{33}^{*}-\varepsilon_{11}^{*}\right)\left[3\eta_1 - \frac{3(7+8\Lambda)\eta_2}{7+5\Lambda}\left(\frac{r}{R}\right)^2\right]\sin 2\theta
\end{aligned}
\tag{19}
$$

and

$$
\begin{aligned}
\sigma_{rr} &= -\frac{2(2+3\Lambda)\chi_1\tau_0}{(5+3\Lambda)R} - \mu\left[\left(\varepsilon_{33}^{*}+\varepsilon_{11}^{*}\right)+\Lambda\left(\varepsilon_{33}^{*}+2\varepsilon_{11}^{*}\right)\right] \\
&\quad - \mu\left\{\frac{2(2+3\Lambda)}{5+3\Lambda}\left(\varepsilon_{33}^{*}+2\varepsilon_{11}^{*}\right)\eta_0 - \left(\varepsilon_{33}^{*}-\varepsilon_{11}^{*}\right)\left[\eta_1 - \frac{3\Lambda\eta_2}{2(7+5\Lambda)}\left(\frac{r}{R}\right)^2\right]\right\} \\
&\quad - \mu\left(\varepsilon_{33}^{*}-\varepsilon_{11}^{*}\right)\left[1-3\eta_1+\frac{9\Lambda\eta_2}{2(7+5\Lambda)}\left(\frac{r}{R}\right)^2\right]\cos 2\theta, \\
\sigma_{\theta\theta} &= -\frac{2(2+3\Lambda)\chi_1\tau_0}{(5+3\Lambda)R} - \mu\left[\left(\varepsilon_{33}^{*}+\varepsilon_{11}^{*}\right)+\Lambda\left(\varepsilon_{33}^{*}+2\varepsilon_{11}^{*}\right)\right] \\
&\quad - \mu\left\{\frac{2(2+3\Lambda)}{5+3\Lambda}\left(\varepsilon_{33}^{*}+2\varepsilon_{11}^{*}\right)\eta_0 - \left(\varepsilon_{33}^{*}-\varepsilon_{11}^{*}\right)\left[\eta_1 - \frac{15\Lambda\eta_2}{2(7+5\Lambda)}\left(\frac{r}{R}\right)^2\right]\right\} \\
&\quad + \mu\left(\varepsilon_{33}^{*}-\varepsilon_{11}^{*}\right)\left[1-3\eta_1-\frac{21(4+5\Lambda)\eta_2}{2(7+5\Lambda)}\left(\frac{r}{R}\right)^2\right]\cos 2\theta, \\
\sigma_{\varphi\varphi} &= -\frac{2(2+3\Lambda)\chi_1\tau_0}{(5+3\Lambda)R} - \mu\left[2\varepsilon_{11}^{*}+\Lambda\left(\varepsilon_{33}^{*}+2\varepsilon_{11}^{*}\right)\right] \\
&\quad - \mu\left\{\frac{2(2+3\Lambda)}{5+3\Lambda}\left(\varepsilon_{33}^{*}+2\varepsilon_{11}^{*}\right)\eta_0 + \left(\varepsilon_{33}^{*}-\varepsilon_{11}^{*}\right)\left[2\eta_1+\frac{3(14+15\Lambda)\eta_2}{2(7+5\Lambda)}\left(\frac{r}{R}\right)^2\right]\right\} \\
&\quad - \mu\frac{3(14+25\Lambda)}{2(7+5\Lambda)}\left(\varepsilon_{33}^{*}-\varepsilon_{11}^{*}\right)\eta_2\left(\frac{r}{R}\right)^2\cos 2\theta, \\
\sigma_{r\theta} &= \mu\left(\varepsilon_{33}^{*}-\varepsilon_{11}^{*}\right)\left[1-3\eta_1-\frac{3(7+8\Lambda)\eta_2}{2(7+5\Lambda)}\left(\frac{r}{R}\right)^2\right]\sin 2\theta,
\end{aligned}
\tag{20}
$$

respectively. It is obvious that the above solution contains the intrinsic length parameters τ_0/μ, μ_0/μ, and λ_0/μ, and hence, is size dependent. Also, the strain and the stress inside the inclusion is non-uniform in the sense that it is dependent on $(r/R)^2$. This result cannot be predicted by the classical elasticity theory.

4. Numerical results and discussion

Apparently, the size dependent nature of elastic field in the inclusion is a result of the strain dependent interface stress, as described in Eq. (2). Indeed, if the interface stress is ignored, i.e., $\tau_0 \to 0$, $\mu_0 \to 0$,

$\lambda_0 \to 0$, the results in Eqs. (18)–(20) will be scaling-invariant. Then, the corresponding r- and θ-components of the displacement, denoted by u_r^0, u_θ^0, in the inclusion will be

$$u_r^0 = r\left[\frac{2(1+\Lambda)}{5(2+\Lambda)}\varepsilon_{33}^* + \frac{4+9\Lambda}{15(2+\Lambda)}\varepsilon_{11}^* + \frac{8+3\Lambda}{15(2+\Lambda)}\left(\varepsilon_{33}^* - \varepsilon_{11}^*\right)\cos 2\theta\right],$$
$$u_\theta^0 = -\left(\varepsilon_{33}^* - \varepsilon_{11}^*\right) r \frac{8+3\Lambda}{15(2+\Lambda)}\sin 2\theta. \tag{21}$$

This is exactly the same as the prediction of classical theory without interface effect. To illustrate the size dependence in a quantitative manner, the difference between u_r, u_θ and u_r^0, u_θ^0 at the interface will be compared. For the description of the interface one needs the constants τ_0, μ_0 and λ_0. Unfortunately, except that interfacial tension τ_0 is known experimentally in some embedded Quantum Dot structures (Wang et al., 1999), the other two interface parameters are currently unavailable in the literature. Miller and Shenoy (2000) have computed free surface for aluminum and silicon by the embedded atom method (EAM), and indicated that the surface properties can be either positive or negative, depending upon crystallographic orientation. According to their results, the absolute values of intrinsic length τ_0/μ, μ_0/μ, λ_0/μ are nearly 0.1 Å, 1.0 Å and 1.0 Å. Although the interface and free surface are not strictly the same, they have similar physical nature (free surface can be regard as some special interface). Since we cannot obtain systematic data of these interface parameters, as a makeshift, in this paper we assume the relevant parameters are basically of the same orders. For convenience, we denote $\delta = 10\tau_0/\mu = \mu_0/\mu = \lambda_0/\mu$. Fig. 2 shows the relative errors between u_r and u_r^0 at $\theta = 0$, u_θ and u_θ^0 at $\theta = \frac{\pi}{4}$, respectively, for various values of inclusion radius, where $\varepsilon_{11}^* = 0$, $\varepsilon_{33}^* = 0.01$, $\Lambda = 1.5$ and $\delta = 1.0$ or -1.0 Å are taken. It can be seen that positive value of δ causes the interface to shrink while negative value of δ causes the interface to dilate. The phenomenon cannot be predicted by the classical elasticity without considering the effect of interface stress. This implies that there exists significant local softening or hardening due to interface effect, as predicted by ab initio calculation (Zhou and Huang, 2004) or continuum model (He et al., 2004) for a free solid surface. It is obvious that interface stress have a considerable influence on u_r than u_θ . For both cases, the relative errors increase with the decrease of the inclusion radius, the size dependence becomes significant only when the inclusion radius is below 10 nm. It should be noted that, with uniform, hydrostatic eigenstrain, i.e., $\varepsilon^*\mathbf{e}_1 \otimes \mathbf{e}_1 + \varepsilon^*\mathbf{e}_2 \otimes \mathbf{e}_2 + \varepsilon^*\mathbf{e}_3 \otimes \mathbf{e}_3$, the θ-component of the displacement, u_θ, inside the inclusion will disappear, and the r-component u_r will be

$$u_r = r\frac{(2+3\Lambda)\mu\varepsilon^* - 2\tau_0/R}{3(2+\Lambda)\mu + (4\mu_0 + 4\lambda_0 + 2\tau_0)/R}. \tag{22}$$

This differs slightly from the following result given by Sharma et al. (2003)

$$u_r = r\frac{(2+3\Lambda)\mu\varepsilon^* - 2\tau_0/R}{3(2+\Lambda)\mu + (4\mu_0 + 4\lambda_0)/R}, \tag{23}$$

in which a term $2\tau_0/R$ is missing in the denominator because the last term in the second equation in Eq. (2) has been omitted.

Due to the effect of interface, the distributions of strain and stress fields within the inclusion also depend on the inclusion radius. An important result due to Eshelby (1957), which has played a key role in the micromechanics of solids, is that for an ellipsoidal inclusion with uniform eigenstrain embedded into an unbounded matrix, the resulting strain within it is also uniform. In particular, a spherical inclusion with the uniform eigenstrain $\varepsilon_{33}^*\mathbf{e}_3 \otimes \mathbf{e}_3$ will lead to the following uniform strain field

$$\varepsilon_{11} = \varepsilon_{22} = -\frac{2-3\Lambda}{15(2+\Lambda)}\varepsilon_{33}^*,$$
$$\varepsilon_{33} = \frac{14+9\Lambda}{15(2+\Lambda)}\varepsilon_{33}^*, \tag{24}$$
$$\varepsilon_{12} = \varepsilon_{13} = \varepsilon_{23} = 0.$$

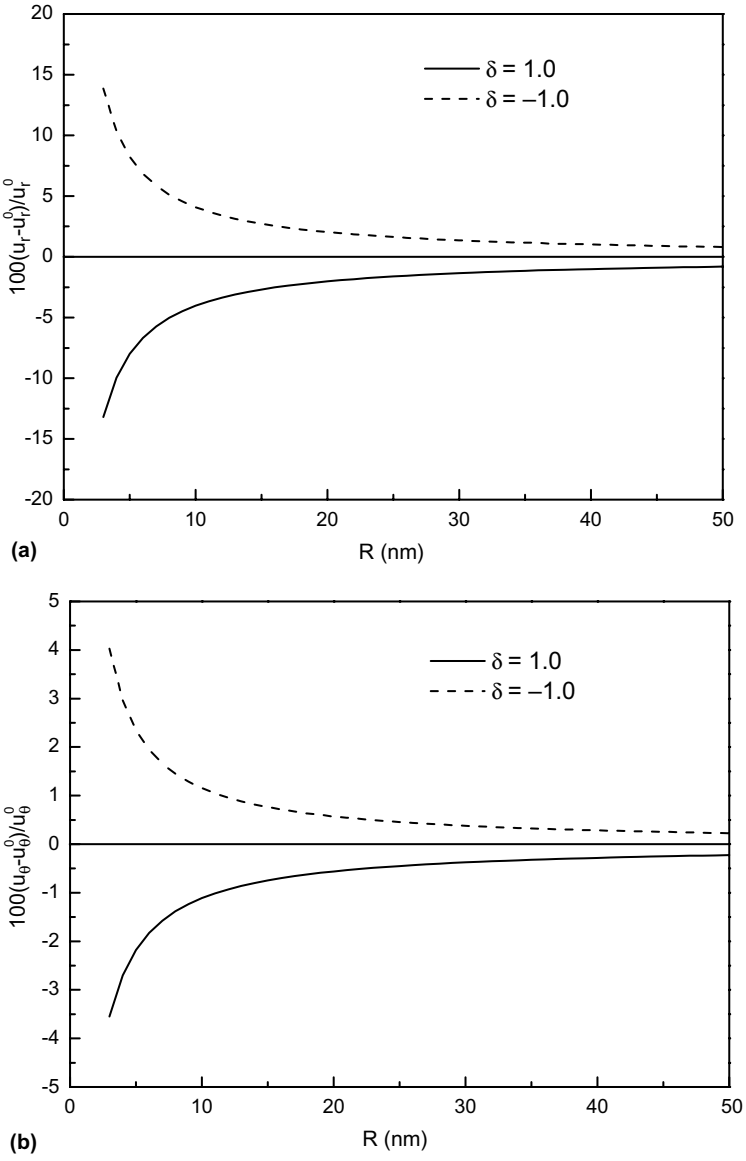

Fig. 2. Relative error of the displacement as a function of inclusion radius: (a) the radial component u_r at $\theta = 0$ and (b) the θ component at $\theta = \frac{\pi}{4}$.

However, in the present work which incorporates the effect of interface stress, the above strain field inside the inclusion will be no longer uniform, but depends on r and θ instead. Numerical results for the distribution of $\varepsilon_{33}/\varepsilon_{33}^*$ inside the inclusion, along the r-direction for $\theta = 0$ and $\theta = \frac{\pi}{2}$, are plotted in Fig. 3, where the inclusion radius $R = 5$ nm and 15 nm are taken for comparison. It can be seen that the magnitude of $\varepsilon_{33}/\varepsilon_{33}^*$ for positive δ is larger than the classical result, while for negative δ the magnitude is smaller. With decreasing inclusion radius, the value of $\varepsilon_{33}/\varepsilon_{33}^*$ decreases for positive δ and increases for negative δ. Along the r-direction, the value of $\varepsilon_{33}/\varepsilon_{33}^*$ decreases for positive δ and increases for negative δ, and reaches the minimum and maximum at the interface (i.e. $r/R = 1$), respectively. A greater variation of $\varepsilon_{33}/\varepsilon_{33}^*$ along the r-direction occurs as the radius of the inclusion decreases. It is also observed that the value of $\varepsilon_{33}/\varepsilon_{33}^*$ is almost the same for different θ. All these facts clearly demonstrate that ε_{33} is not only size dependent, but also non-uniform inside the inclusion. On the other hand, for uniform, hydrostatic eigenstrain, $\varepsilon^*\mathbf{e}_1 \otimes \mathbf{e}_1 + \varepsilon^*\mathbf{e}_2 \otimes \mathbf{e}_2 + \varepsilon^*\mathbf{e}_3 \otimes \mathbf{e}_3$, the resulting strain

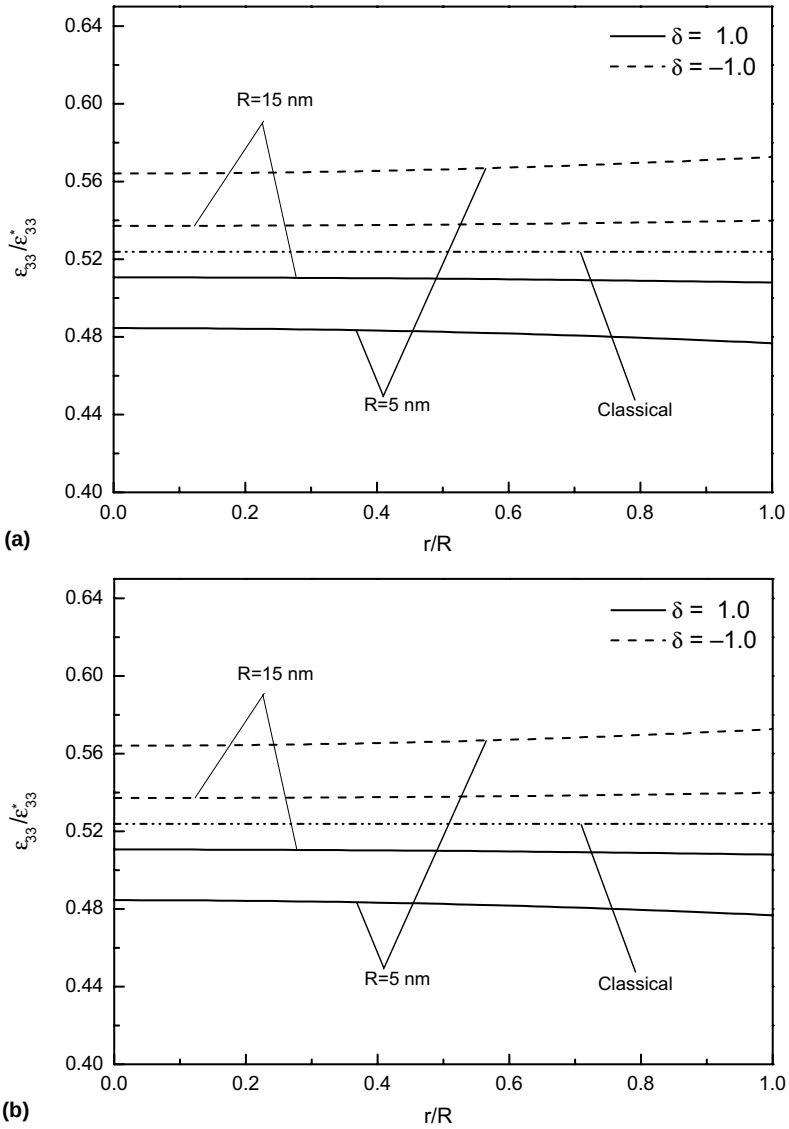

Fig. 3. Distribution of strain component ε_z along the r-direction inside the inclusion: (a) $\theta = 0$ and (b) $\theta = \frac{\pi}{2}$.

$$\varepsilon_{11} = \varepsilon_{22} = \varepsilon_{33} = \frac{(2+3\Lambda)\mu\varepsilon^* - 2\tau_0/R}{3(2+\Lambda)\mu + (4\mu_0 + 4\lambda_0 + 2\tau_0)/R} \tag{25}$$

will be still uniform within the inclusion, but it depends on the inclusion radius.

5. Conclusion

Incorporating the interface effect, an analytical solution for a spherical inclusion embedded in an infinite matrix with uniform, non-hydrostatic eigenstrain is derived and discussed. The solution concludes that the strain state of the elastic system is size dependent, differing significantly from the classic result obtained from the classical linear elasticity. Numerical computation indicates that such a size dependence is quite remarkable when the radius of the inclusion is below tens of nanometer. Different elastic constants of the interface may cause the interface to either shrink or dilate, implying that there exists local softening or hardening at the interface of the inclusion and the matrix. Another important conclusion is that interface stress results in non-uniform elastic

field inside the spherical inclusion when the eigenstrain is non-hydrostatic even if uniform. These results indicate that interface stress plays a significant role in the elastic behavior of embedded inclusions of nano-scale size.

Acknowledgement

The work described in this paper was supported by YSS Funding of the City University of Hong Kong.

Appendix. Expressions of the dimensionless in Eq. (14)

The dimensionless constants ξ_0, ξ_1, ξ_2, η_0, η_1, η_2, χ_0 and χ_1 in Eq. (14) are defined by

$$\begin{aligned}
&\xi_0 = A_0\eta_0, \quad \xi_1 = A_1\eta_1 + A_2\eta_2,\\
&\xi_2 = A_3\eta_3 + A_4\eta_4, \quad \chi_0 = A_0\chi_1,\\
&\eta_0 = \frac{B_0}{3+\gamma_0}, \quad \eta_1 = \frac{B_1+\beta_1}{525+\gamma_1},\\
&\eta_2 = \frac{\beta_2}{525+\gamma_1}, \quad \chi_1 = \frac{B_2}{3+\gamma_0},
\end{aligned} \tag{A.1}$$

$$\begin{aligned}
&A_0 = \frac{2}{5+3\Lambda}, \quad A_1 = \frac{3(1+\Lambda)}{8+3\Lambda},\\
&A_2 = \frac{5(7+8\Lambda+3\Lambda^2)}{(8+3\Lambda)(7+5\Lambda)},\\
&A_3 = \frac{5}{8+3\Lambda}, \quad A_4 = \frac{21(1+\Lambda)}{(8+3\Lambda)(7+5\Lambda)},\\
&B_0 = -\frac{(5+3\Lambda)(2+3\Lambda)}{6(2+\Lambda)},\\
&B_1 = \frac{70(8+3\Lambda)}{3(2+\Lambda)},\\
&B_2 = \frac{5+3\Lambda}{2+\Lambda}.
\end{aligned} \tag{A.2}$$

$$\begin{aligned}
\beta_1 &= \frac{8(8+3\Lambda)(7+3\Lambda)}{(2+\Lambda)^2}\frac{\lambda_0}{\mu R} + \frac{112(8+3\Lambda)}{3(2+\Lambda)}\frac{\mu_0}{\mu R}\\
&\quad + \frac{8(14+\Lambda)}{3(2+\Lambda)}\frac{\tau_0}{\mu R},\\
\beta_2 &= \frac{8(8+3\Lambda)(7+5\Lambda)}{3(2+\Lambda)^2}\frac{\lambda_0+2\mu_0-\tau_0}{\mu R},\\
\gamma_0 &= \frac{4\lambda_0+4\mu_0+2\tau_0}{(2+\Lambda)\mu R},\\
\gamma_1 &= \frac{2\lambda_0}{\mu R}\left[\frac{5(112+33\Lambda)}{3(2+\Lambda)} + \frac{4(8+3\Lambda)(7+5\Lambda)}{3(2+\Lambda)^2}\frac{2\mu_0+\tau_0}{\mu R}\right]\\
&\quad + \frac{2\mu_0}{\mu R}\left[\frac{35(28+9\Lambda)}{3(2+\Lambda)} + \frac{4(8+3\Lambda)(7+5\Lambda)}{3(2+\Lambda)^2}\frac{2\mu_0+5\tau_0}{\mu R}\right]\\
&\quad + \frac{2\tau_0}{\mu R}\left[\frac{5(98+27\Lambda)}{3(2+\Lambda)} - \frac{4(8+3\Lambda)(7+5\Lambda)}{3(2+\Lambda)^2}\frac{\tau_0}{\mu R}\right].
\end{aligned} \tag{A.3}$$

References

Bimberg, D., Grundmann, M., Ledentsov, M.N., 1999. Quantum Dot Heterostructures. John Wiley & Sons, Chichester.

Eshelby, J.D., 1957. The determination of the elastic field of an ellipsoidal inclusion and related problems. Proceedings of Royal Society A 241, 376–396.

Goodier, J.N., 1933. Concentration of stress around spherical and cylindrical inclusions and flaws. Journal of Applied Mechanics 55, 39–44.

Gurtin, M.E., Murdoch, A., 1975. A continuum theory of elastic material surfaces. Archives of Rational Mechanics Analysis 57, 291–323.

Gurtin, M.E., Weissmuller, J., Larche, F., 1998. A general theory of curved deformable interfaces in solids at equilibrium. Philosophical Magazine A 78, 1093–1109.

He, L.H., Lim, C.W., Wu, B.S., 2004. A continuum model for size-dependent deformation of elastic films of nano-scale thickness. International Journal of Solids and Structures 41, 847–857.

Love, A.E.H., 1944. Mathematical Theory of Elasticity. Dover Publications, New York, Netherlands.

Miller, R.E., Shenoy, V.B., 2000. Size-dependent elastic properties of nanosized structural elements. Nanotechnology 11, 139–147.

Mura, T., 1987. Micromechanics of Defects in Solids. Martinus-Nijhoff, Netherlands.

Rose, K.C., Wang, J., Hutchinson, J.W., Lieber, C.M., 2000. Nanoplate mechanics: dramatic decrease in young's modulus, unpublished.

Sharma, P., Ganti, S., 2002. Interfacial elasticity corrections to size-dependent strain-state of embedded quantum dots. Physique Status Solida B 234, R10–R12.

Sharma, P., Ganti, S., 2004. Size-dependent Eshelby's tensor for embedded nano-inclusions incorporating surface/interface energies. Journal of Applied Mechanics 71, 663–671.

Sharma, P., Ganti, S., Bhate, N., 2003. Effect of surfaces on the size-dependent elastic state of nano-inhomogeneities. Applied Physics Letters 82, 535–537.

Sun, C.T., Zhang, H., 2003. Size-dependent elastic moduli of platelike nanomaterials. Journal of Applied Physics 93, 1212–1218.

Sun, L., Wu, Y.M., Huang, Z.P., Wang, J.X., 2004. Interface effect on the effective bulk modulus of a particle-reinforced composite. Acta Mechanica Sinica 20, 676–679.

Wang, L.G., Kratzer, P., Scheffler, M., Moll, N., 1999. Formation and stability of self-assembled coherent islands in highly mismatched heteroepitaxy. Physical Review Letters 82, 4042–4045.

Wong, E., Sheehan, P.E., Lieber, C.M., 1997. Nanobeam mechanics: elasticity, strength, and toughness of nanorods and nanotubes. Science 277, 1971–1975.

Yang, F.Q., 2004. Size-dependent effective modulus of elastic composite materials: spherical nanocavities at dilute concentrations. Journal of Applied Physics 95, 3220–3516.

Zhou, L.G., Huang, H., 2004. Are surfaces elastically softer or stiffer? Applied Physics Letters 84, 1940–1942.